Effect of microstructure heterogeneity shapes on constitutive behaviour of encapsulated self-healing cementitious materials

Sayadi, Sina; Ricketts, Evan; Schlangen, Erik; Cleall, Peter; Mihai, Iulia; Jefferson, Anthony

Important note
To cite this publication, please use the final published version (if applicable).
Please check the document version above.

Effect of microstructure heterogeneity shapes on constitutive behaviour of encapsulated self-healing cementitious materials

Sina Sayadi[1]*, *Evan* Ricketts[1], *Erik* Schlangen[2], *Peter* Cleall[1], *Iulia* Mihai[1], *Anthony* Jefferson[1]

[1]School of Engineering, Cardiff University, Cardiff, CF24 3AA, UK
[2]Faculty of Civil Engineering and Geosciences, TUDelft, Delft 2628 CN, The Netherlands

Abstract. Self-healing cementitious materials with microcapsules are complex multiscale and multiphase materials. The random microstructure of these materials governs their mechanical and transport behaviour. The actual microstructure can be represented accurately with a discrete lattice model, but computational restrictions mean that the size of domain that can be considered with this approach is limited. By contrast, a smeared approach, based on a micromechanical formulation, provides an approximate representation of the material microstructure with low computational costs. The aim of this paper is to compare simulations of a microcapsule-based self-healing cementitious system with discrete-lattice and smeared-micromechanical models, and to assess the relative strengths and weaknesses of these models for simulating distributed fracture and healing in this type of self-healing material. A novel random field generation technique is used to represent the microstructure of a cementitious mortar specimen. The meshes and elements are created by the triangulation method and used to determine the input required for the lattice model. The paper also describes the enhancement of the TUDelft lattice model to include self-healing behaviour. The extended micromechanical model considers both microcracking and healing. The findings from the study provide insight into the relative merits of these two modelling approaches.

1 Introduction

To reduce the environmental impact of repairing and maintaining conventional concrete structures, scientists have developed self-healing technologies in cementitious materials [1]. For almost two decades, researchers have investigated different self-healing technologies [2], [3] studying their effects on overall system responses. Many efforts have been devoted to formulating and modelling the physical and chemical processes behind self-healing phenomena [3], and due to their complex coupled behaviour, further research is needed to achieve a robust model.

In the current literature, microencapsulation techniques have been explored as an autonomous self-healing method [4, 5], for example, the specific triggering mechanisms for microcapsule rupture [6, 7]. The relationship between mechanical properties of both shell and matrix has also been investigated to ensure that capsule rupture would occur. Similarly, the probability of a crack intersecting with the shell of a microcapsule has also been investigated, both theoretically and numerically [8]. Rather than considering just the local capsule dynamics, the effects of microcapsules on mechanical properties can be extrapolated to the full system. For example, a homogenization scheme can be employed to estimate the overall representation of the elastic properties of encapsulated cementitious composite materials [9]. Recently, researchers have explored the mechanical recovery of self-healing action in self-healing systems equipped with microcapsules [10]. By adopting a smeared approach, a constitutive formulation was developed to capture the mechanical behaviour of self-healing process [11]. Through using the micromechanical technique, Davies and Jefferson [11] developed a constitutive relationship which can model the distinct healing and re-damaging phases of self-healing systems. Few studies exist which formulate the self-healing effect on mechanical recovery at the element level.

Often, microstructure heterogeneity and its effects on self-healing processes are neglected when modelling. Numerically, explicit representations of concrete mesostructures are generally obtained through aggregate particle placing methods [12], with many models using idealised ellipsoidal shapes [13]. Similar models exist for more realistic structural generation [14, 15], but have high computational costs. A less explored application in cementitious materials is that of discrete random field generation, such as Plurigaussian simulation [16]. The computationally efficient method is highly flexible in the structures it can generate and can produce structures similar to those seen in particulate media.

In the present study, the self-healing responses derived from two different approaches are presented. The effects of cracking and healing on overall mechanical properties are compared. The presence of randomly distributed irregular inclusions on mechanical

---

properties is investigated and compared for different homogenization schemes.

Section 2 presents the model methodologies; Section 3 describes the numerical test case chosen for investigating the healing effect on the mechanical properties of encapsulated systems; Section 4 presents and discusses the results of the simulations; and Section 5 gives the main conclusions of the study.

2 Methodology

The lattice beam element model (LBM) is based on employing multiple beam elements with different properties to represent the microstructure of encapsulated cementitious samples. The micromechanical homogenization approach is also used for developing a constitutive formulation for the distributed crack-healing problem. With this framework, the whole microstructure, including changes due to microcracking and healing, are homogenized as an equivalent medium.

2.1 Smeared approach

The microencapsulated cementitious material consists of a cement paste matrix and microcapsule inclusions. Cracks are considered to be randomly distributed penny shaped cracks. The additional strain caused by microcracking is accounted for in the constitutive formulation related to continuum damage mechanics (CDM)

$$\boldsymbol{\sigma} = \mathbf{D}(\boldsymbol{\varepsilon} - \boldsymbol{\varepsilon}_{\text{add}}) \qquad (1)$$

where $\boldsymbol{\sigma}$ is the average far field stress vector, $\boldsymbol{\varepsilon}$ is the far field prescribed strain, and $\boldsymbol{\varepsilon}_{\text{add}}$ is the additional strain due to the microcracking in global coordinate, and $\mathbf{D}$ is the material stiffness matrix.

The healing effect is considered by adding its effect on each local crack plane. By using the hierarchical homogenization scheme and Budiansky & O'Connell's approach [17], this gives the overall representation of the composite self-healing systems, as illustrated in Fig.1.
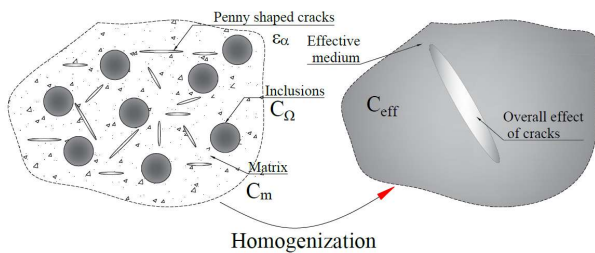

Fig. 1. Schematic illustration for homogenization and microcracking effect

2.1.1 Elastic properties of multiphase composite

The average elastic modulus of a multiphase composite system is derived by employing the classical Eshelbian formulation in combination with Mori-Tanaka estimation [18] for a non-dilute distribution of inclusions of spherical shape. The following equation gives the effective elastic compliance of the two-phase composite system

$$\mathbf{D}_{\text{eff}} = \mathbf{D}_{\mathbf{m}} + (f_{\Omega}(\mathbf{D}_{\boldsymbol{\Omega}} - \mathbf{D}_{\mathbf{m}})\mathbf{A}_{\boldsymbol{\Omega}})(f_m \mathbf{I} + f_{\Omega} \mathbf{A}_{\boldsymbol{\Omega}})^{-1} \quad (2)$$

where $\mathbf{D}_{\text{eff}}$, $\mathbf{D}_{\mathbf{m}}$ and $\mathbf{D}_{\boldsymbol{\Omega}}$ are effective stiffness, matrix stiffness and the inclusions stiffness respectively. f_m and f_{Ω} are the matrix and inclusion volume fractions. $\mathbf{I}$ is the identity tensor and $\mathbf{A}_{\boldsymbol{\Omega}}$ is the dilute strain concentration tensor calculated by

$$\mathbf{A}_{\boldsymbol{\Omega}} = [\mathbf{I} + \mathbf{SC}_{\mathbf{m}}(\mathbf{D}_{\boldsymbol{\Omega}} - \mathbf{D}_{\mathbf{m}})]^{-1} \qquad (3)$$

where $\mathbf{S}$ is the Eshelby tensor related to the inclusion geometry. Finally, $\mathbf{C}_{\mathbf{m}}$ is the matrix elastic compliance, denoted as $\mathbf{C}_{\mathbf{m}} = \mathbf{D}_{\mathbf{m}}^{-1}$.

2.1.2 Crack-healing formulation

The effect of microcracks appears as an additional strain. Budiansky & O'Connell's method is used for calculating the additional strain due to microcracks and its effect on the overall stiffness matrix. As before, cracks are assumed to be penny shaped and randomly distributed throughout the medium. Equation (4) shows the constitutive formulation of distributed microcrack in quasi-brittle materials

$$\boldsymbol{\sigma} = \left(\mathbf{I} + \frac{\mathbf{D}_{\text{eff}}}{2\pi} \oiint_{\Omega} \mathbf{N}_{\boldsymbol{\varepsilon}}^{\mathrm{T}} \mathbf{C}_{\mathrm{L}} \frac{\omega}{1-\omega} \mathbf{N}\right)^{-1} \mathbf{D}_{\text{eff}} \boldsymbol{\varepsilon} \qquad (4)$$

where $\mathbf{N}$ is the transformation matrix, and ω is the damage parameter of the matrix.

The evolution of the damage parameter is determined using an exponential formulation proposed by Jefferson and Bennett [19], which represents degradation in cementitious materials. The effect of the microcracks in each direction on the total response is calculated using an integration over a hemisphere for a representative volume element.

The healing contribution is added on a crack plane stress-strain formulation with a particular orientation as noted in equation 5

$$\mathbf{s}_{\mathrm{Lh}} = (1-\omega)\mathbf{D}_{\mathrm{L}}\boldsymbol{\varepsilon}_{\mathrm{L}} + h_v \mathbf{D}_{\mathrm{Lh}}(1-\omega_h)(\boldsymbol{\varepsilon}_{\mathrm{L}} - \boldsymbol{\varepsilon}_{\mathrm{h}}) \quad (5)$$

where $\mathbf{S}_{\mathrm{Lh}}$ is stress vector on crack plane, $\mathbf{D}_{\mathrm{L}}$ and $\mathbf{D}_{\mathrm{Lh}}$ are the original and healed material stiffness matrix respectively, ω_h is the damage parameter of the healed material, $\boldsymbol{\varepsilon}_{\mathrm{h}}$ is the healed material offset strain which ensures that healing happens in a stress-free condition, and h_v is the amount of healed material which can be associated with time. The healing rate can be described mathematically via the exponential function $(1 - e^{t/\tau})$, where τ represents the healing rate constant.

The total additional strain due to microcracking and healing for the whole representative material is derived by rearranging the equation (5) and substituting into equation (1). The simultaneous effect of damage and healing shows itself in overall stiffness and the offset strain. During a healing process, the energy should be constant. This criterion should be maintained by introducing an offset strain in global coordinates. The derivation of healed secant stiffness as well as global offset strain for satisfying thermodynamic conditions in constitutive formulation would be fully discussed in the forthcoming journal paper. Fig.2 presents the normalized constitutive responses of this formulation for uniaxial tensile test loading-unloading scenarios. To have a schematic representative behaviour for healing in brittle materials, the derived overall stresses and strains are divided to the assumed original material maximum tensile strengths and corresponding tensile strain respectively to provide a dimensionless curve. The healing initiation time is noted figure. It is assumed that three different of healing agent with different healing rate time is used.
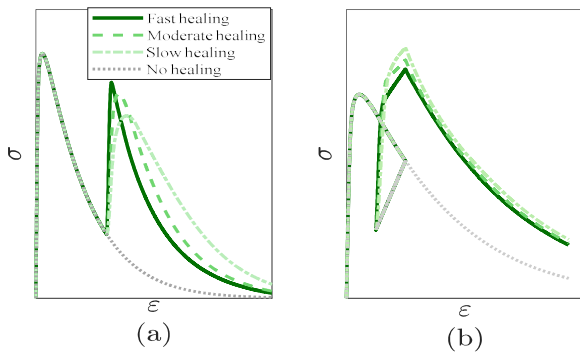

Fig.2. Uniaxial tension constitutive response of self-healing composite material for: a) monotonic loading, b) loading-unloading case

2.2 Lattice approach

The discrete nature of the LBM allows crack propagation to be tracked in analyses. The cracking process is captured by removing the damage element and updating the local and global stiffness matrices. Healing events are also considered by recovering the damaged element in the deformed condition. The system stiffness and local forces would be updated during the healing step. Similarly, the microstructure can be accounted for by discretising the structural domain into sets of randomly distributed nodes and elements. A brief overview of the lattice mesh generation and cracking-healing formulation are presented below.

2.2.1 Lattice structure generation

The domain is discretised with beam elements which connect a set of randomly positioned nodes and is generated using a Delaunay triangulation algorithm. Only elements with the common Voronoi face are considered, whose element cross-sectional area is calculated based on the Voronoi facet area. Fig.3. illustrated how the lattice meshes are generated.
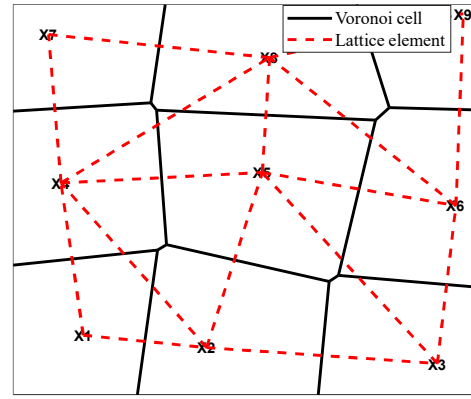

Fig. 3. Schematic illustration of triangulation Delaunay

2.2.2 Self-healing process in lattice method

Here, healing processes are simulated by retrieving the damaged element during the recovery phase (Fig.4). At a healing step, based on the healed material properties for a given healed element, the stiffness matrix is updated and the overall structural matrix is reassembled.
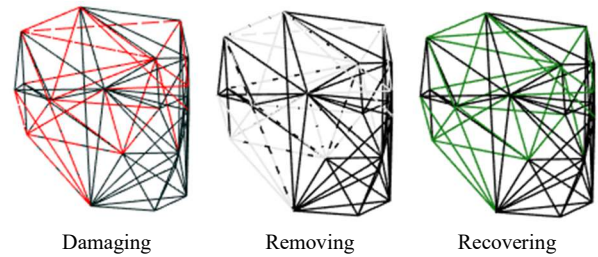

Fig. 4. Removal and recovery mechanism proposed in the Lattice method.

The healed element length and coordinates are also updated based on the deformed state at the time of healing. In the same step, the local force-displacement equation and global equilibrium equation is adjusted such that no energy is created, meaning that the nodal force before and after the healing step will be the same. The nodal healing adjustment displacement is defined in a way that the nodal force before healing step where just stiffness matrix is updated due to healing, and after healing step are the same. The algorithm and derivation of this step is elaborated in the forthcoming journal paper.

2.3 Microstructure generation

2.3.1 Irregular inclusion distribution

Plurigaussian simulation is employed to generate the distribution of aggregate particles. Let $\{Z_1, Z_2\}$ be a set of two independent random fields in $\mathbb{R}^2$, and define a random field $\boldsymbol{Z}$ where:

$$\boldsymbol{Z}(\mathbf{x}) = \big(Z_1(\mathbf{x}), Z_2(\mathbf{x})\big), \quad \forall \mathbf{x} \in \mathbb{R}^2. \tag{11}$$

Let $L = \{D_1, \ldots, D_m\}$ be a partition of $\mathbb{R}^2$ into m disjoint subdomains, such that the plurigaussian random field $\boldsymbol{P}$ with m distinct facies can be defined as:

$$P(\mathbf{x}) = i \Leftrightarrow Z(\mathbf{x}) \in D_i, \quad \forall \mathbf{x} \in \mathbb{R}^2. \tag{12}$$

In principle, two (or more) Gaussian random fields are truncated using a prescribed lithotype rule to attain a discrete map which represents the desired phases, here being matrix and aggregate particle. In this case, we also apply a convex hull operation to the generated field P to create shapes synonymous with aggregate particles, as seen in Figures 5 and 6.

2.3.2 Random computational microcapsules generation.

A pixel-based framework is used for the aggregate phase to determine microcapsule geometry and location. The shape of the microcapsules is created by using the Bresenham algorithm [20], which rasterizes the shell of the microcapsules in the pixel-based domain. The centre of each capsule is chosen such that there is no overlap between neighbouring microcapsules and aggregate particles. The proposed algorithm randomly distributed microcapsules within the composite cementitious domain, illustrated in red in Fig.5 for differing volume fractions.
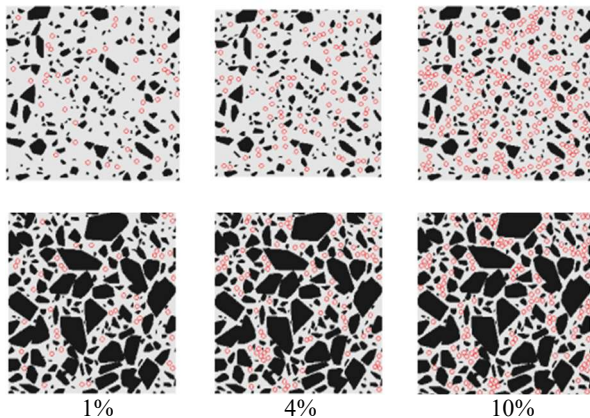

Fig. 5. Samples generated structures for different volume fractions and microcapsule inclusion percentage.

3 Example

A typical cementitious mortar with 33% aggregate and 2.5 % microcapsules inclusion is considered to examine how self-healing affects the response of a uniaxial tensile test. The sample 2D domain has dimensions 4 cm × 4 cm, where the loading rate is assumed to be 0.0001mm/sec (0.000025mm/mm/sec for the strain path) such that healing would be initiated when the applied boundary displacement is reached at 0.075 mm. Here, it is assumed that healing has happened instantaneously.

The Mori-Tanaka approach is employed to derive the elastic properties of the RVE in the smeared method, and constitutive response is derived according to the method described in section 2.1.

The material mechanical properties and geometry is presented in Table 1 and Fig.6 respectively.

Table 1. Material mechanical properties.

Material /Properties	$v_f\%$	E(GPa)	f_t(MPa)	ε_t
Matrix-interface	33.0	30	4	0.00015
Aggregate	63.5	49	-	-
Microcapsules	2.5	0.03	0.1	-
Healing agent	-	30	3.0	0.00015

The parameter ε_t noted in Table 1 is the microcracking strain parameter used for the micromechanical model. In the lattice approach, the total number of nodes and elements are chosen appropriately such that the assumed mesh can capture the microstructure features as well as the crack propagation.
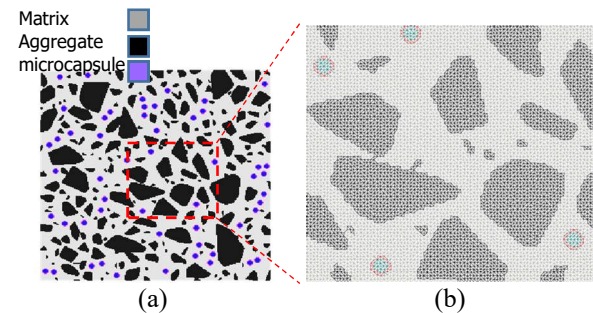

Fig. 6. Considered RVE for: a) computational microstructure, b) Lattice mesh in the highlighted region.

In this study it is assumed that the bond between microcapsules and cement is perfect. It is also assumed that a given capsule ruptures when it is intersected by a propagating crack. To compare the crack pattern with and without healing, the system was solved for both scenarios.

4 Results

The calculated responses derived from the two proposed method are presented in Fig. 7. The slope of the force-displacement curve indicates that the overall stiffness of the RVE calculated from both the Lattice and smeared method are quite the same. Fig. 7 Shows the stress-strain relation for smeared and Lattice approaches with and without healing process. The comparison of the crack pattern between the control sample and healing cases illustrated in Fig.8. It shows that after healing the newly formed crack is different form the reference sample at the same stage.
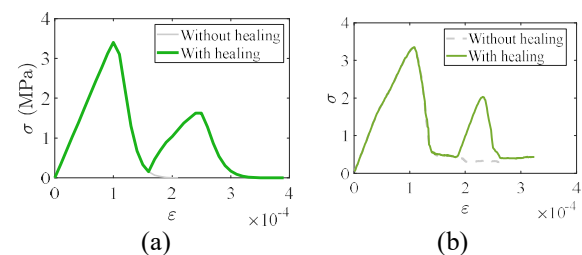

Fig. 7. Uniaxial responses, a) smeared approach, b) discrete approach
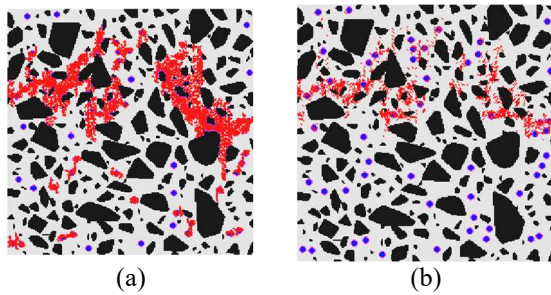
(a)   (b)

Fig. 8. Crack pattern, a) damage only, b) cracks after healing

It is worth noting that to represent the microstructure explicitly, 65000 elements were needed. Consequently, the computational costs were relatively high compared to the smeared approach.

5 Conclusions

The effects of self-healing on the mechanical response of heterogeneous cementitious materials have been studied. The constitutive behaviour and explicit modelling have been undertaken by extending existing micromechanical and discrete lattice models. Through using the combination of Plurigaussian simulation and the modified Bershams rasterising algorithm, the microstructure of encapsulated cementitious materials is generated. The main conclusions are as follows:

- The micromechanical formulation can capture the full elastic and nonlinear responses of self-healing materials
- The effect of multiphases and their interactions with cracking and healing can be modelled explicitly by Lattice method. Healing effects can alter crack propagation paths
- The computational costs of the smeared approach are much less than those of the Lattice method.

References

1.   K. van Tittelboom and N. de Belie, *Materials*, vol. 6, no. 6, (2013)

2.   L. Ferrara *et al.*, *Constr Build Mater*, vol. 167. pp. 115–142, (2018)

3.   T. Jefferson, E. Javierre, B. Freeman, A. Zaoui, E. Koenders, and L. Ferrara," *Adv. Mater*, vol. 5, no. 17, p. 1701378, (2018)

4.   C. Litina and A. Al-Tabbaa, *Constr Build Mater*, vol. 255, (2020)

5.   C. Xue, W. Li, J. Li, V. W. Y. Tam, and G. Ye, suco, vol. 20, no. 1, (2019)

6.   L. Y. Lv, H. Zhang, E. Schlangen, Z. Yang, and F. Xing, *Constr Build Mater*, vol. 156, (2017)

7.   F. A. Gilabert, D. Garoz, and W. van Paepegem, *Mater Des*, vol. 130, pp. 459–478, (2017)

8.   S. v Zemskov, H. M. Jonkers, and F. J. Vermolen, *Comput Mater Sci*, vol. 50, no. 12, pp. 3323–3333, (2011)

9.   W. Li, Z. Jiang, Z. Yang, and H. Yu,Mater Des, vol. 95, pp. 422–430, (2016)

10.   K. Han, J. W. Ju, H. Zhang, Y. Zhu, T.-S. Chang, and Z. Wang, *Constr Build Mater*, vol. 280, p. 122251, (2021)

11.   R. Davies and A. Jefferson, *Int J Solids Struct*, vol. 113–114, pp. 180–191, (2017)

12.   P. S. M. Thilakarathna, K. S. Kristombu Baduge, P. Mendis, V. Vimonsatit, and H. Lee, *engfracmech*, vol. 231, p. 106974, May (2020)

13.   X. Li, Y. Xu, and S. Chen, *Constr Build Mater*, vol. 121, pp. 100–111, Sep. (2016)

14.   J. Zhang, Z. Wang, H. Yang, Z. Wang, and X. Shu, *Constr Build Mater*, vol. 164, pp. 350–361, Mar. (2018)

15.   V. Holla, G. Vu, J. J. Timothy, F. Diewald, C. Gehlen, and G. Meschke, *Materials*, vol. 14, no. 14, p. 3782, (2021)

16.   M. Armstrong *et al.*, *Plurigaussian Simulations in Geosciences*. Berlin Springer Berlin, (2014).

17.   B. Budiansky and R. J. O'Connell, *Int J Solids Struct*, vol. 12, no. 2, pp. 81–97, (1976)

18.   A. D. Jefferson and T. Bennett, *Comput Struct*, vol. 88, no. 23, pp. 1361–1366, (2010)

19.   A. Jefferson and T. Bennett, *Num. Anal. Meth. Geomech.* , vol. 31, pp. 133–146, (2007)

20.   J. E. Bresenham, *IBM Systems Journal*, vol. 4, no. 1, (2010)